Available online at www.sciencedirect.com

ScienceDirect

Journal of Electrical Systems and Information Technology 1 (2014) 234–254

www.elsevier.com/locate/jesit

Comparative study of 250 W high pressure sodium lamp operating from both conventional and electronic ballast

Ahmed A. Mansour*, Osama A. Arafa*

Electronics Research Institute, DokKi, Cairo, Egypt

Available online 19 December 2014

Abstract

Bulky electromagnetic ballasts combined with igniters have been traditionally used to feed high pressure sodium lamps (HPS). Recently electronic ballasts were introduced to perform the same tasks more efficiently and even with additional features like dimming and smart energy saving. This paper presents a comparative study of the operational characteristics of a 250 W HPS lamp when fed by conventional ballast versus electronic ballast. The operational characteristics are obtained in both cases through direct measurements on two commercial setups in which the only difference is the ballast type. The comparison study covers both warming period and steady state or nominal power operation. This comparative study gives solid numerical evidences of the superior performance of the electronic over the conventional ballast.

Keywords: HPS lamp; Electromagnetic ballast; Electronic ballast; Comparative study

1. Introduction

Since the early 1970s, the high pressure sodium lamp, has become one of the most important light sources for outdoor lighting thanks to its high luminous efficacy (about 140 lm/W), good color rendering via its golden white color appearance and long lamp life (24,000–32,000 h; Sincero et al., 2005). In high pressure discharging lamps, lamp exhibits negative impedance characteristics and its impedance moves from very large value to a very small value upon gas breakdown therefore auxiliary devices are necessary to generate high breakdown voltage for startup and then to stabilize lamp current by absorbing the differential voltage between the line and the lamp once the discharge arc is well established.

Abbreviations: HPS, high pressure sodium lamp; HPM, high pressure metal halide lamp; CB, conventional ballast; EB, electronic ballast; PFC, power factor correction; ZVS, zero voltage switching; ZCS, zero current switching; THD, total harmonic distortion.

* Corresponding authors.

E-mail addresses: mansour@eri.sci.eg (A. A. Mansour), arafa@eri.sci.eg (O. A. Arafa).

Peer review under the responsibility of Electronics Research Institute (ERI).

Production and hosting by Elsevier

http://dx.doi.org/10.1016/j.jesit.2014.12.006

Main applications of the high intensity discharge lamp are usually found in the street lighting, stadium, highways, industrial lighting, and airport lighting.

The economic crisis all overall the world in recent years has stimulated energy saving concerns and a strong tendency to preserve natural resources has arisen. Many new technologies have been applied to the traditional electrical equipment in order to improve their efficiency. Lighting was no exception; intensive research has been carried out to replace the bulky and low efficiency conventional electromagnetic ballasts with light weight high efficiency electronic ballasts. For low-watt fluorescent lamp, the electronic ballast industry and markets have been growing rapidly. But the electronic ballasts usage for high intensity discharge lamp (HPS and HPM) grows slowly. This is partially due to some technical issues and mainly due to debatable cost-benefits trade-offs.

In Martín et al. (2010), a spectroscopic comparative study was conducted to investigate the behavior of HPS lamp when it is fed by 50 Hz and high frequency (40–63 kHz) mains. The voltages at which these lamps worked when they were stabilized were 88 V for 50 Hz, and 60–62 V (r.m.s.) for high frequencies. These voltages were determined by the electronic conditions of ignition ballasts. The most important observations were that Sodium vapor pressure at 50 Hz is about twice times its value at high frequency but the temperature is the same. This implies that longer lamp life time can be realized with high frequency operation.

It has been shown that at high frequency operation, HPS lamp acts as a constant pure resistive load (Branas et al., 1998), that is independent of power level and operating frequency within the range 27–75 kHz (Ben-Yaakov and Gulko, 1997) and such resistance can be doubled along lamp life time due to aging (Branas et al., 1998), hence active power control is necessary to maintain lamp power constant along its life time. Another feature related to aging is that the sufficient level of ignition voltage is likely to increase with aging of the lamp, thus a careful design should provide sufficient ignition voltage to avoid ignition failure during useful lamp life (Cardesin et al., 2003).

Since its early introduction in 1980 (Dorleijn and Vanderheijden, 1980), electronic ballasts for HID lamps have been introduced in a wide variety of topologies and designs each of which has its own pros and cons.

Typically electronic ballasts employ two-stage power conversion where the first stage can be a buck converter to take care of power factor correction and the second stage can be a resonant tank containing the lamp and fed through a full bridge inverter to take care of feeding the lamp at high frequency as in Cardesin et al. (2003). Full-bridge inverter stage itself has been proposed in many variants; one of those smart variants is the series-parallel resonant inverter as in Branas et al. (2000) that satisfies many operational requirements like soft ignition at no extra cost, minimizing the volt-ampere of feeding the lamp and adaptive power control to limit lamp power diminishing due to aging.

However, single stage topologies were introduced also; they mainly address cost reduction and have been proposed in different configurations as well (Martin et al., 2003; Florian Giezendanner et al., 2014). In Martin et al. (2003) it combines a boost converter with a resonant inverter and it does not require additional ignition circuitry. This design could offer a PFC feature therefore the main advantage of such topology is high reliability due to merging the two typical stages in one stage thus reducing component count and the very low inverter losses due to switching the MOSFETs at certain points along the waveform (ZVS, ZCS). In Florian Giezendanner et al. (2014) Electronic ballasts for high-pressure sodium lamps based on single-stage AC-chopper topology proposed as a cheaper and less complex alternative to the industry-standard low-frequency square-wave ballasts

In Jeong et al. (2001) single stage topology is offered as a half-bridge inverter operating a series resonant tank for both igniting and continuous lamp operation while it ignores the PFC issue. In Branas et al. (1998) it is proposed as a half-bridge parallel resonant converter.

The control parameter used to vary the output power in all single stage topologies is the switching frequency; hence they are basically variable frequency methods in which higher frequency results in lower power delivered to the lamp. In two-stage topologies a combination of duty ratio and switching frequency control have been used to achieve the superior performance.

Some other techniques have been also reported like AC chopper (Sincero et al., 2005) to make benefits of fewer components count and design compactness yet achieving high power factor and low total harmonic distortion of the input current.

In light of the current energy crisis in Egypt, the purpose of the study is however not to assess performance superiority among different electronic ballast designs but to compare the operational characteristics of a 250 W HPS lamp when fed by a commercial medium-priced electronic ballast with their corresponding characteristics when it is fed through a commercial CB which is the dominant case in most Egyptian public lighting systems. To do this we study three different feeding systems:

- The lamp is fed at 50 Hz through a CB with no power factor correction capacitor.
- The lamp is fed at 50 Hz through a CB with power factor correction capacitor.
- The lamp is fed by an arbitrary selected medium priced commercial EB.

The paper is organized as follows: Section 2 presents the first system, Section 3 presents the second system, the third system is presented in Section 4 and Section 5 gives a comparison between CB and EB operational profiles. The conclusion of the study is given in Section 6 followed by a list of references.

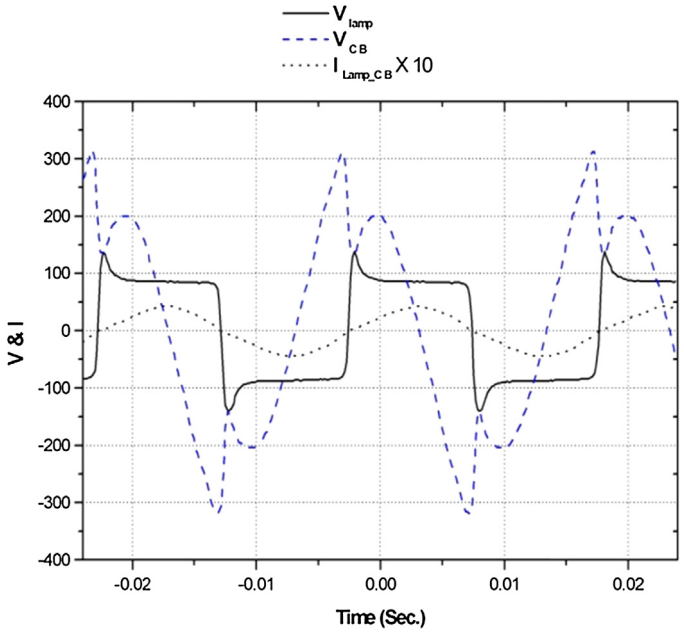

Fig. 1. Instantaneous waveforms for CB.

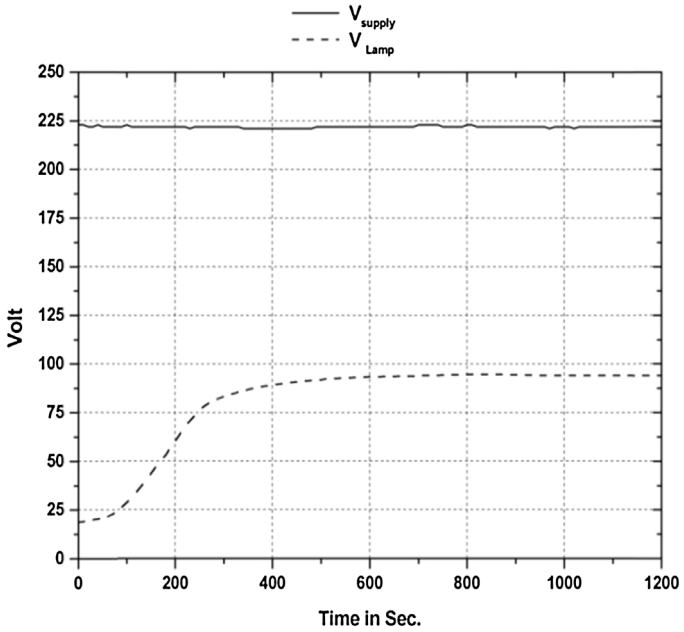

Fig. 2. Lamp voltage V_{lamp}.

2. Conventional ballast without PFC

The operation of the HPS 250 W lamp using the conventional ballast is presented in the next set of Figs. 1–9. Fig. 1 shows the instantaneous waveforms of CB voltage, lamp voltage, and the lamp current. The conventional ballast system draws sinusoidal current. Lamp voltage appears as a lightly distorted square waveform, and ballast voltage appears as heavily distorted sinusoidal voltage. This shows that at low frequency operation, the lamp has quite non-linear but resistive nature as current and voltage waveforms share same polarity and their zero crossings coincide.

Fig. 2 shows the lamp behavior form start-up through the warming up period till it reaches its steady state operation.

Figs. 2 and 3 show that at a supply r.m.s. voltage of about 222 V the lamp reaches its steady state operation after nearly 10 min. The lamp's voltage and current start at 19 V, 3.74 A and ends at steady state at 94 V, 3.06 A respectively (all in r.m.s. values).

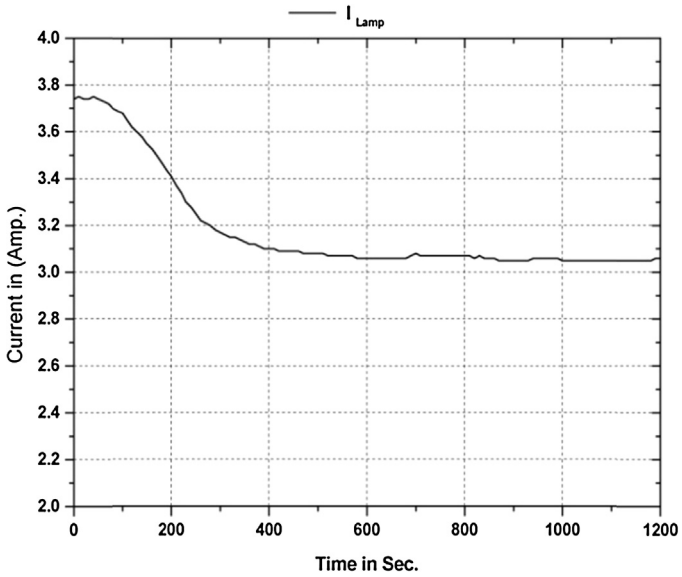

Fig. 3. Lamp current I_{lamp}.

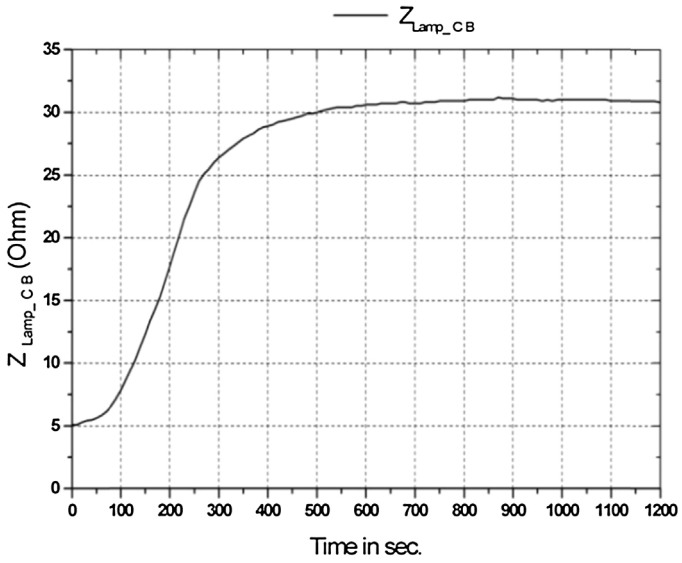

Fig. 4. Lamp impedance Z_{lamp}. Electronics Research Institute.

Fig. 4 shows that immediately upon gas breakdown the lamp gets a definite positive resistance of 5 Ω and grows exponentially till it reaches a steady state value of 31 Ω.

Fig. 5 shows that the CB system starts the 250 W HPS lamp at power level of 68 W while the input power at the supply end is 116 W with a net power loss of 48 W. Lamp's power grows to reach 245 W at steady state. Input power at the supply end in this case is 280 W with a net power loss of 36 W. The decrease in power loss is attributed mainly to the decrease in the lamp's current magnitude and its I^2R losses of the CB winding, hence the power loss profile shown in Fig. 5 is somehow tracking the lamp's current profile of Fig. 3

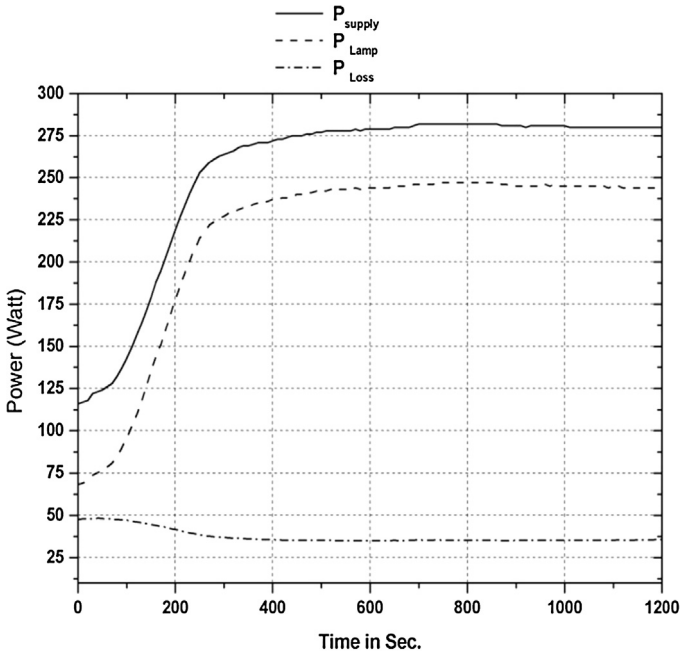

Fig. 5. Power curves for CB system.

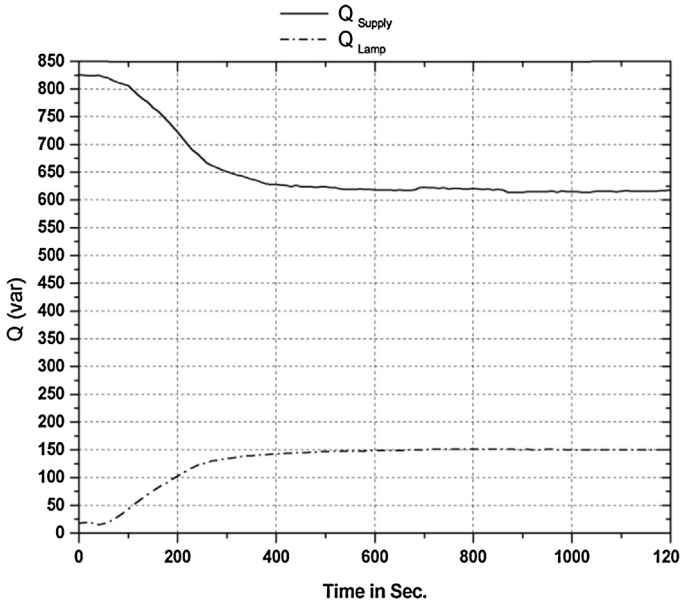

Fig. 6. Reactive power of the CB system.

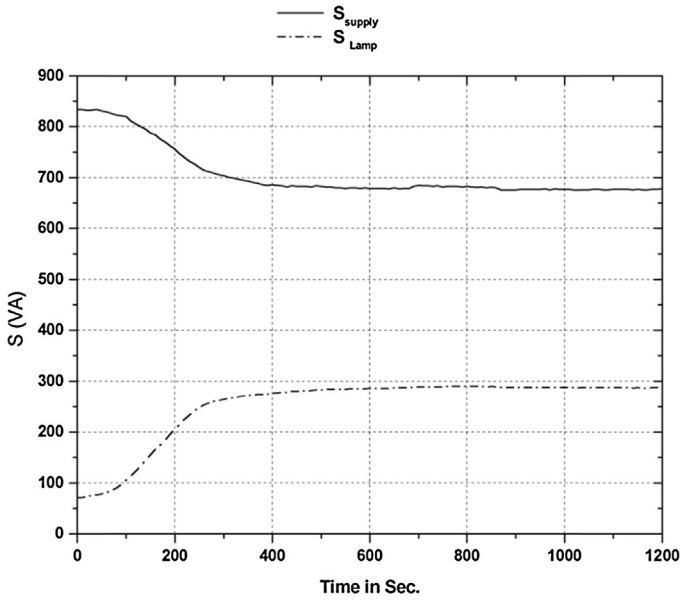

Fig. 7. Apparent power of the CB system.

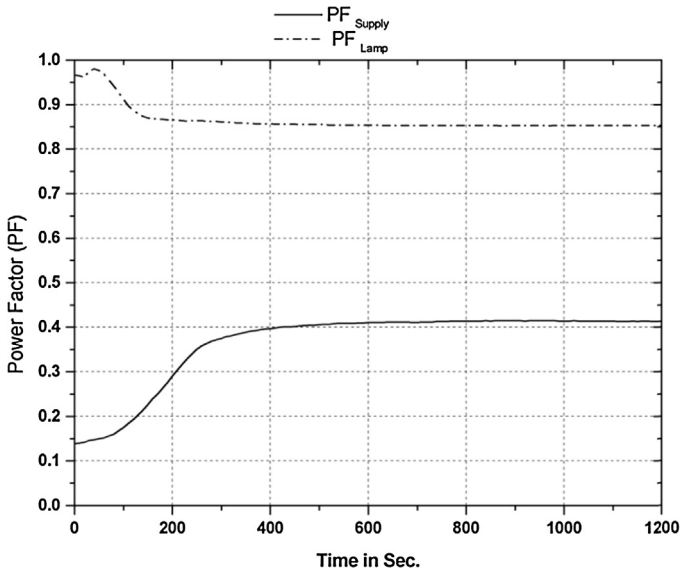

Fig. 8. Power factor of the CB system.

Fig. 6 shows the reactive power measured across the HPS lamp and across the supply. It is noticed that the CB system circuit draws a highly reactive power of 825 VAR at starting due to the high CB coil inductance and the low HPS lamp resistance which is 5 Ω. After warming period elapses, the lamp resistance builds up to 31 Ω as shown in Fig. 4. The increased overall circuit impedance and the reduced overall impedance angle result in reducing the total reactive power to about 617.7 VAR.

For the lamp itself, although the lamp acts as a pure resistance, it draws reactive harmonic power following the same change in the profile of the lamp resistance due to its nonlinear resistive characteristics at this low frequency which results in increased harmonic voltage content across the lamp.

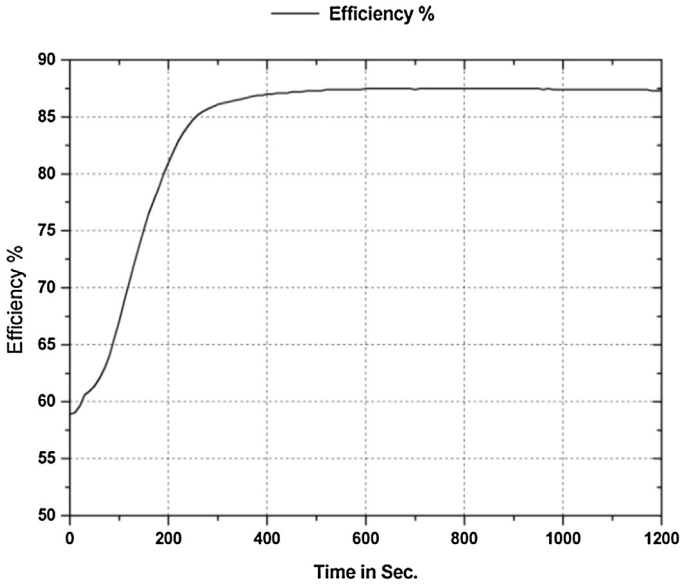

Fig. 9. Efficiency of the CB system.

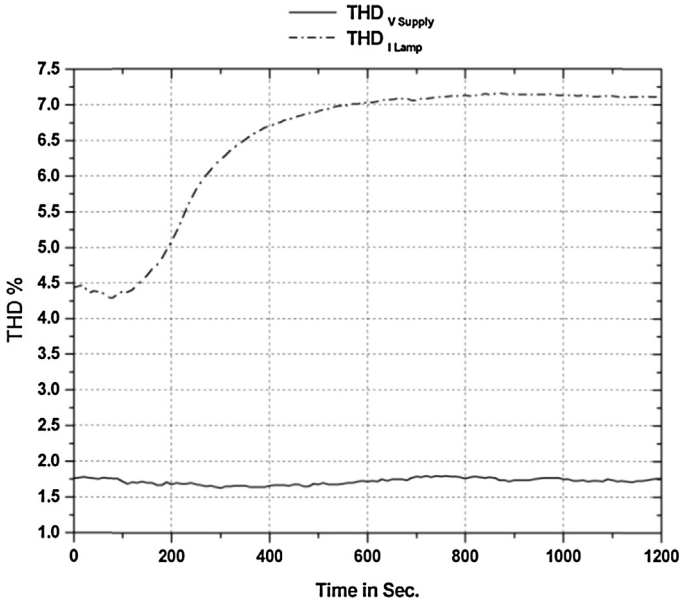

Fig. 10. THD of the CB system.

Fig. 7 shows the steady state apparent power drawn across both supply and HPS lamp. It is clear that without PFC capacitor, the apparent power is very high and reaches 678.3 VA, also the lamp terminal apparent power is about 287 VA.

Fig. 8 shows the power factor at the supply point as well as the PF at the lamp point. The PF at the supply starts at about 0.15 and ends at about 0.413. The lamp power factor starts very close to unity but drops to 0.853 at steady state due to the lamp's growing non-linear resistance that draws harmonic power as explained in the previous paragraph.

Fig. 9 shows the efficiency profile of the system of the CB and the lamp with a start-up efficiency of 58% and a steady state efficiency of 87.31%.

Fig. 10 shows the supply total harmonic distortion (THD) is 1.75% and THD_i is nearly 7% for supply current.

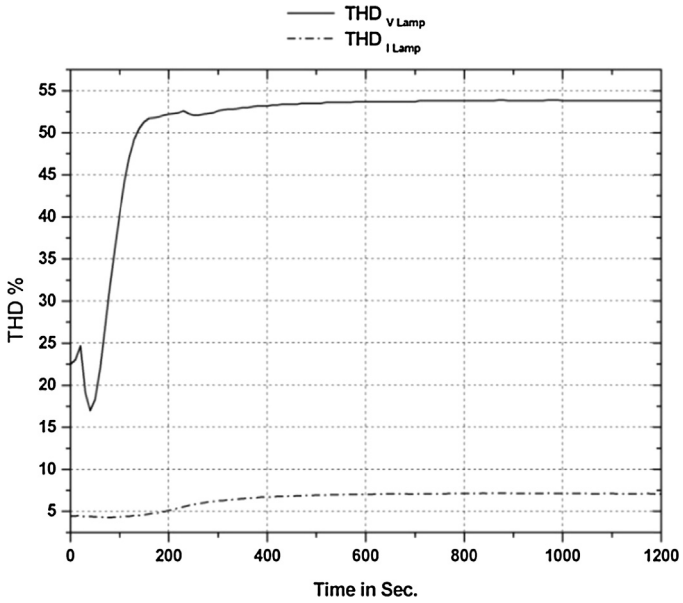

Fig. 11. THD lamp voltage and current.

Also, Fig. 11 shows $THD_{V\_lamp} = 53.7\%$ at the lamp terminals. This is again in line with the explanation given in the previous paragraphs regarding harmonic voltage generated by the increased magnitude of the lamp's nonlinear resistance which has reflections in the THD of the current drawn by the system as well.

3. Conventional ballast with PFC

With power factor correction capacitor $C_{PF} = 35\ \mu F$, 250 V connected at the load point (i.e. the series combination of CB and the 250 W HPS lamp), Fig. 12 shows that the total reactive power drawn from the supply is reduced to

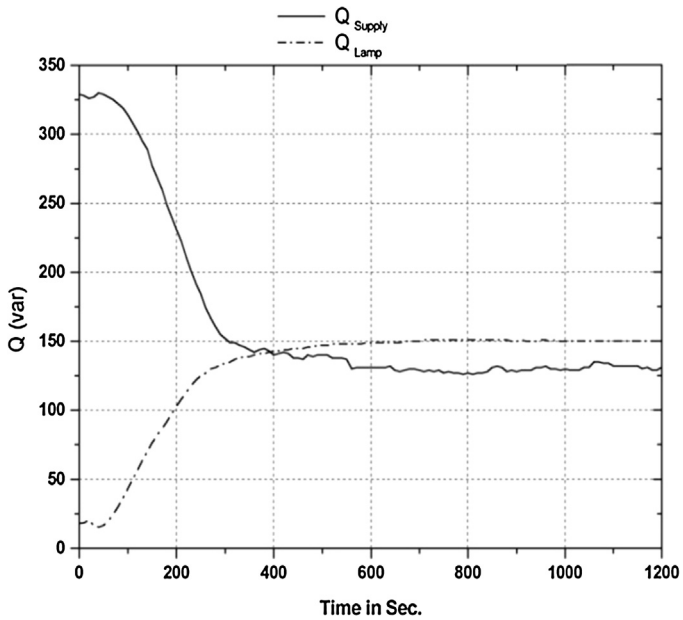

Fig. 12. Reactive power Q (VAR).

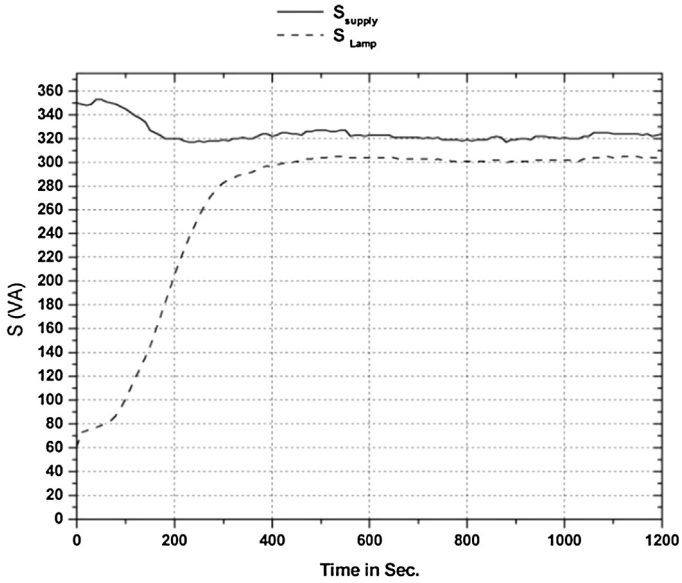

Fig. 13. Apparent power in (VA).

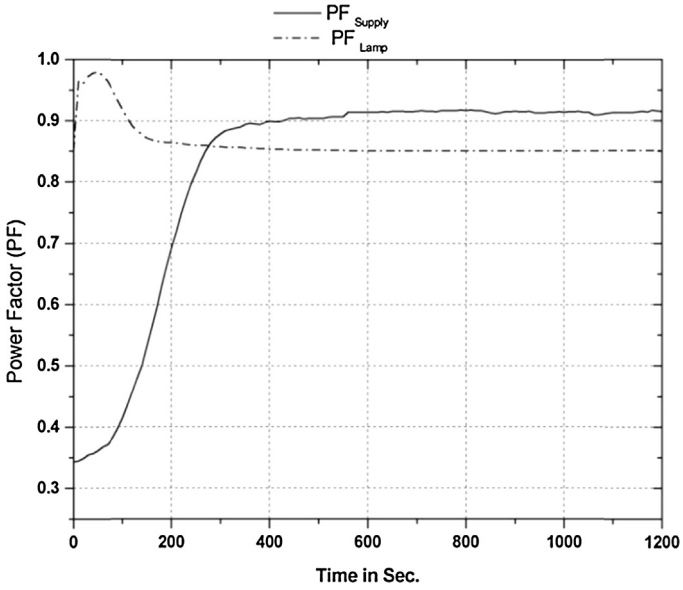

Fig. 14. Power factor.

130.7 VAR at steady state. As expected C_{PF} does not alter the inherent nonlinear characteristics of the lamp itself, therefore the lamp reactive power profile remains unchanged and similar to that of Fig. 6.

Figs. 13 and 14 show that at steady state the total apparent power drawn from the supply is reduced to 323.7 VA and the supply power factor is improved to 0.915, respectively. Again C_{PF} does not affect the PF profile of the lamp.

The salient disadvantage of power factor correction capacitor is an observable increase in the total harmonic distortion of the supply current. THD of I_{sup} reaches 30% as shown in Fig. 15

In fact this observation thus worded is misleading somehow; what actually happens is that a considerable proportion of the supply current recorded in the case of CB with no capacitor (it is 90 degree lagging the supply voltage) is contributing to the denominator of the THD ratio thus results in a low THD. Adding a power factor correction capacitor eliminates the lagging component by the an anti-phase current component drawn by the power factor correction capacitor

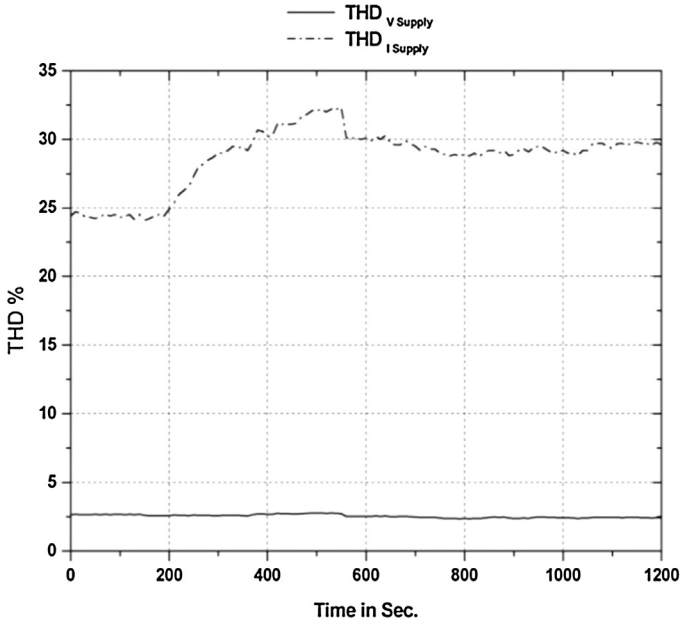

Fig. 15. Total harmonic distortion.

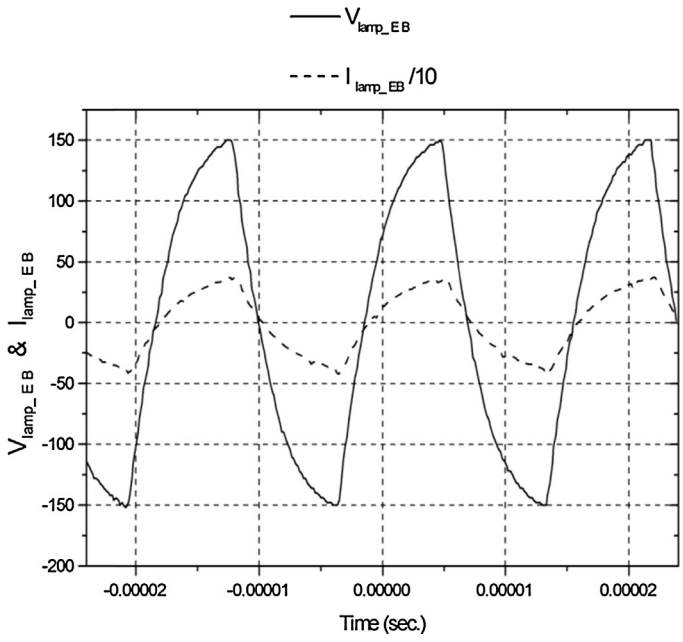

Fig. 16. EB instantaneous waveforms.

(90 degree leading the supply voltage) thus reduces the magnitude of the supply current and minimizes the denominator of the THD ratio while the nominator represented by the harmonic distortion in the lamp current as portrayed in Fig. 10 is left unchanged. Thus the masking effect of the CB-alone highly reactive current previously understating the impact of the lamp harmonic distortion in the supply current is reduced to a minimum leaving the lamp harmonic distortion fully exposed and reflected in the THD of the assembly when fitted with C_{PF}.

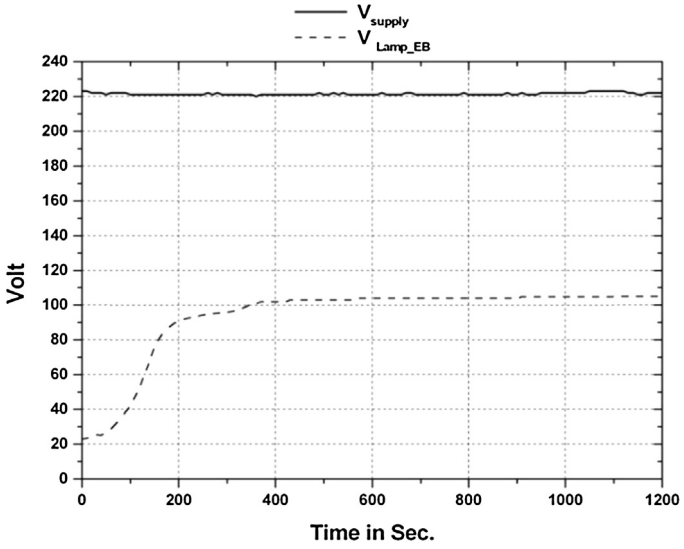

Fig. 17. Lamp voltage V_{lamp}.

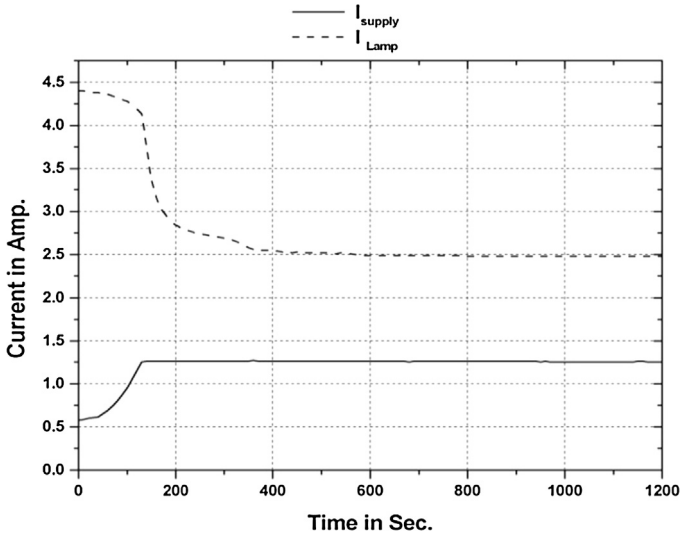

Fig. 18. Lamp and supply current using EB.

4. Electronic ballast

The EB behavior is introduced in this section. It should be understood that apart from the charachetersitcal feature of having the lamp acting as a pure and relatively linear resistance changing only with the discharge arc temperature in high frequency excitation mode, the timings and some operational values shown in the following set of figures is attributed to active and pre-programmed control algorithm embedded in the microcontroller of the EB more than being attributed to inherent characteristics of the lamp itself. Fig. 16 shows the instantenous output voltage and current waveforms at operating frequency 58.8 kHz. Both voltage applied to the lamp and its current are symmetrical and in time phase. Thus ensuring that the lamp represents a pure resistive load with high linearity at high operating frequency.

Fig. 17 shows lamp voltage when operating from EB. The lamp reaches a steady state voltage of about 102 V within 400 s.

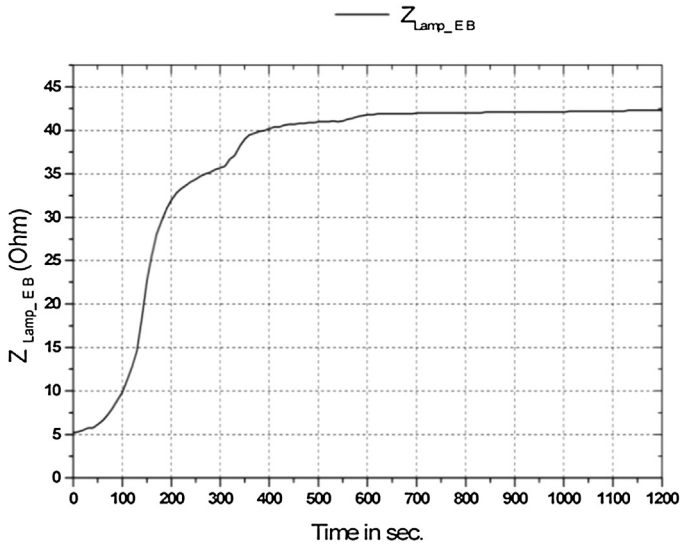

Fig. 19. Lamp impedance behavior.

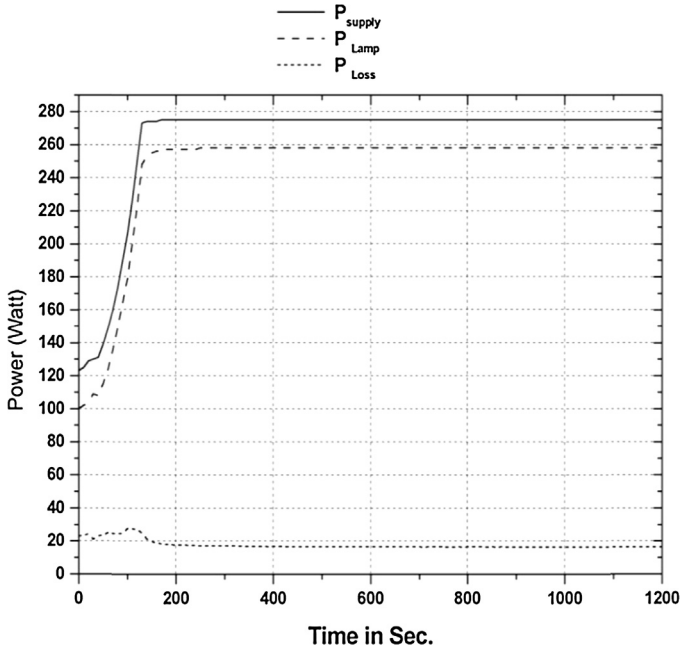

Fig. 20. EB system power consumptions.

Fig. 18 shows that upon ignition, the lamp current starts at 4.4 A. It reaches 2.5 A at steady state within 475 s. Also, the corresponding supply current starts with 0.57 A then reaches 1.26 A within 120 s i.e. before the lamp reaches steady state operation.

After HPS lamp ignition succeeds, the lamp impedance shown in Fig. 19 starts at 5.1 Ω, and increases during the warming-up period until it reaches a steady value 42 Ω, these values represent lamp characteristics at high frequency excitation and at the corresponding arc temperatures.

Fig. 20 shows the power consumptions where the lamp starts drawing power equal to 100 W till it reaches its rated power within 120 s. The EB loss starts at 23 W due to the lamp's high starting current as shown in Fig. 18 (increased turn on losses of the electronic switches contributes to this loss). As the lamp current decreases the corresponding EB power loss is decreased and reaches a steady value of 17 W.

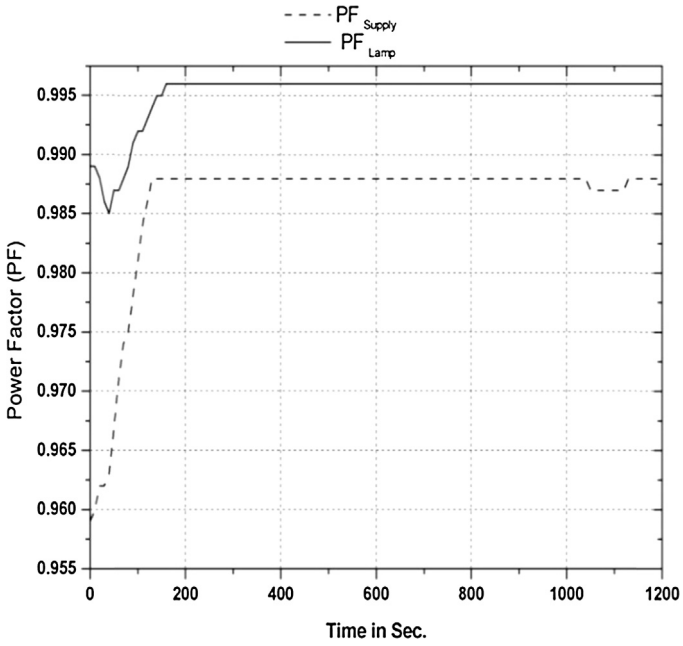

Fig. 21. Power factor using EB.

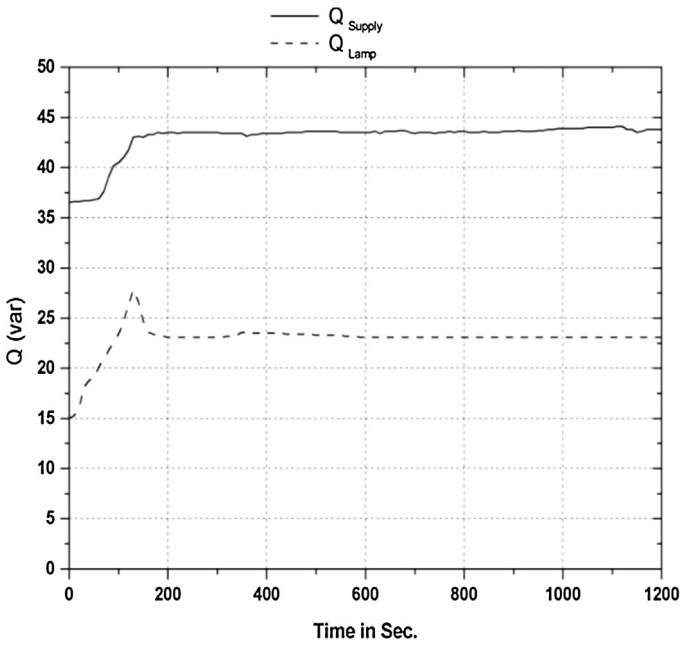

Fig. 22. Reactive power Q of EB system.

Using EB system improves the power factor at the supply point to 0.988 as shown in Fig. 21. Also the lamp power factor is improved to 0.996 due to improving the lamp linearity by using high frequency excitation.

Fig. 22 shows that the total reactive power at the supply point is 44 VAR and at the lamp terminals is 23 VAR at steady state.

Fig. 23 shows the total apparent power at the supply point and at the lamp as 278 VA and 260 VA respectively at steady state.

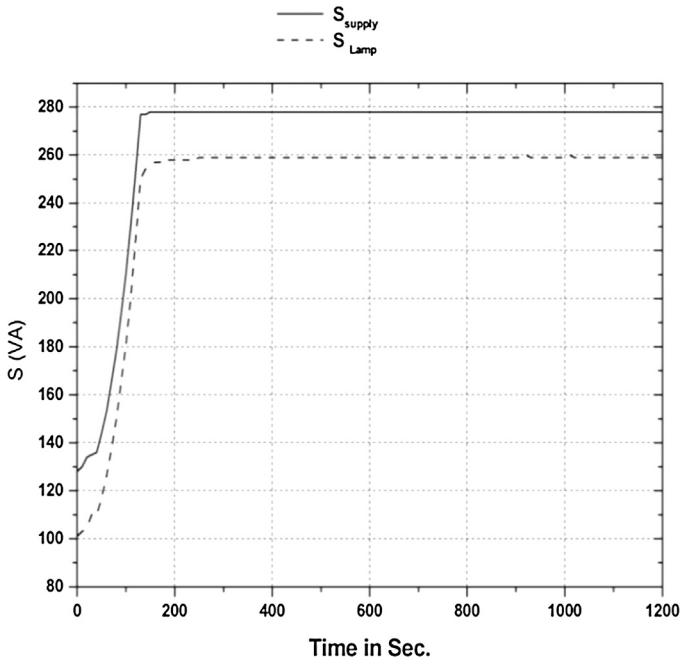

Fig. 23. Apparent power of EB system.

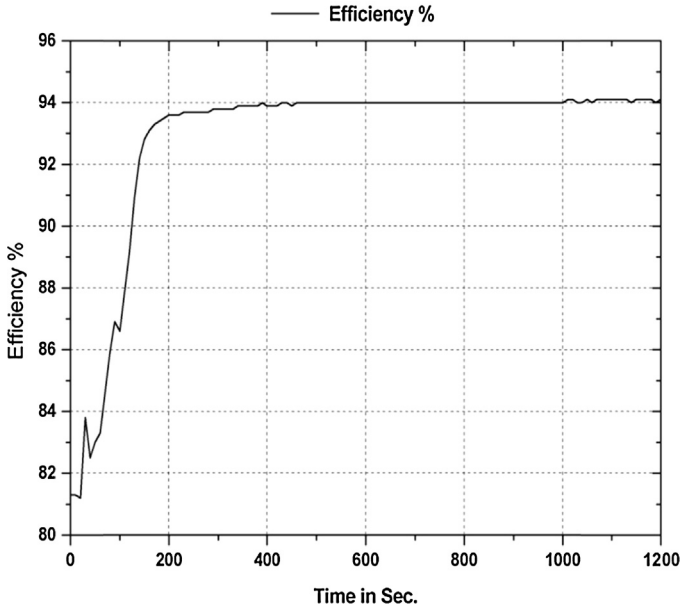

Fig. 24. Efficiency of EB system.

Fig. 24 shows the efficiency of the EB system driving 250 W HPS lamp. The steady state efficiency slightly exceeds 94%.

5. Comparison between EB and conventional ballast

This section is dedicated to comparing side by side the lamp operational parameters upon ignition till steady state on both feeding systems. We will refer to feeding the lamp through CB by case 1 and to feeding it by EB as case 2.

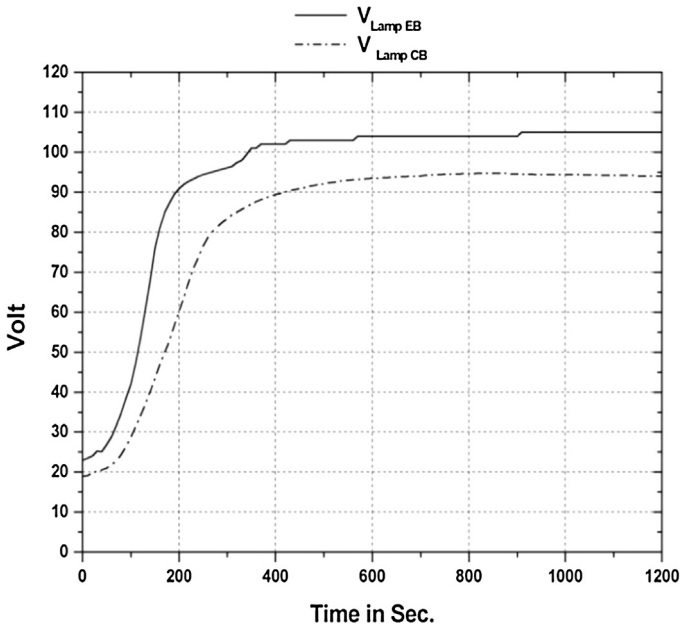

Fig. 25. Lamp voltage under both CB and EB

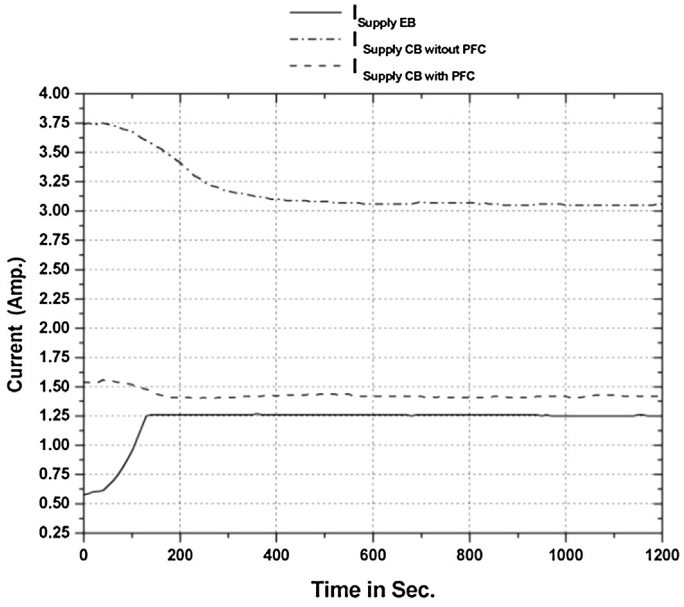

Fig. 26. Supply lamp currents comparison.

Fig. 25 shows that the 250 W HPS lamp voltage starts at 19 V in case 1 versus 23 V in case 2. The steady state lamp voltage reaches 94 V in case 1 versus 105 V in case 2. This is quite contradicting to what is mentioned in Martín et al. (2010) regarding the lamp voltage when fed by high frequency source. Also, it is noted that the warm-up period in case 2 is much shorter than that of case 1 (about 50%) thanks to the active power control facilitated by the EB which utilizes lamp characteristic in a way that optimizes lamp performance.

Fig. 26 shows that case 2 offers the lowest starting and steady state supply current which are 0.57 A and 1.26 A respectively also, the lamp's warming up period is shorter than case 1. Although the supply current in case 1 is considerably reduced by adding a power factor correction capacitor (starting: 1.54 A versus 3.75 A and steady state:

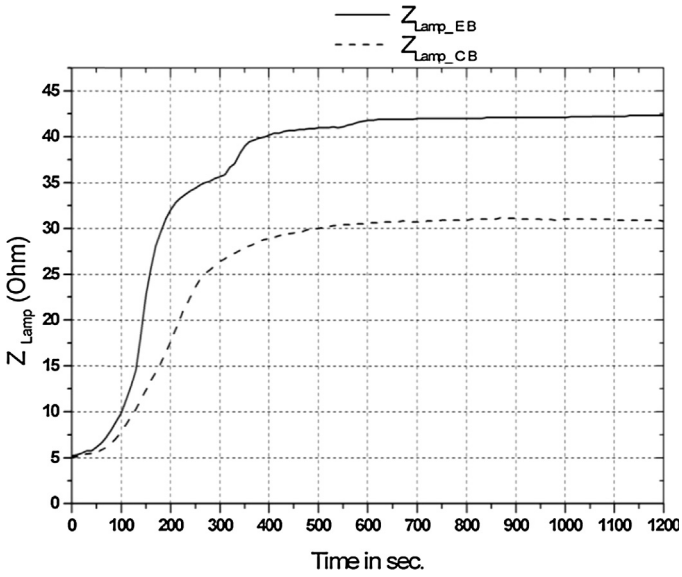

Fig. 27. Lamp impedance both CB and EB.

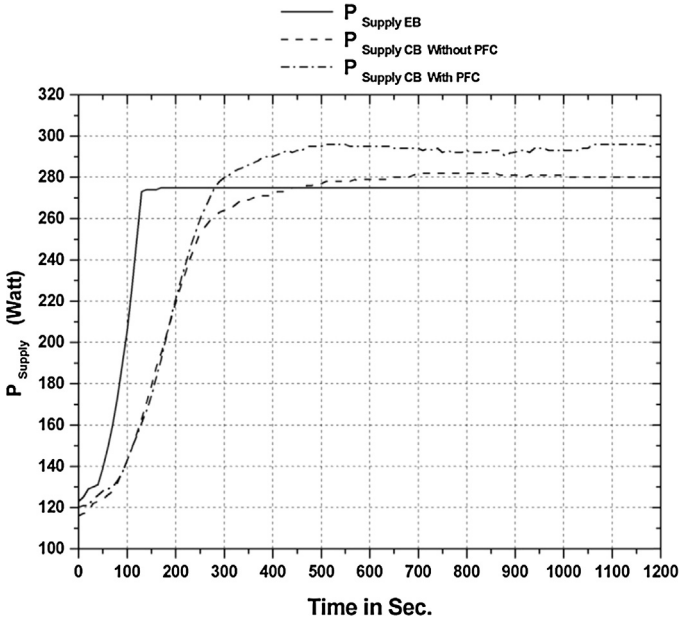

Fig. 28. Power at the supply terminal for both CB and EB.

1.4 A versus 3.4 A), EB still outperforms this assembly even if C_{PF} is assumed as a perfect performance aging-free component.

Fig. 27 shows that the lamp impedance after lamp ignition starts at nearly 5.1 Ω in both cases and changes more rapidly under EB operation. The steady state value is 31 Ω in case 1 and 42 Ohm in case 2.

As for active power at the supply terminal, Fig. 28 shows that case 2 provides superior performance than case 1 in warming up period where it can transfer more active power to the lamp thus shortening that period. In steady state operation it gives same lamp performance using less total input wattage. A secondary effect of the PFC capacitor is shown in the form of additional input power when compared with the case of no capacitor.

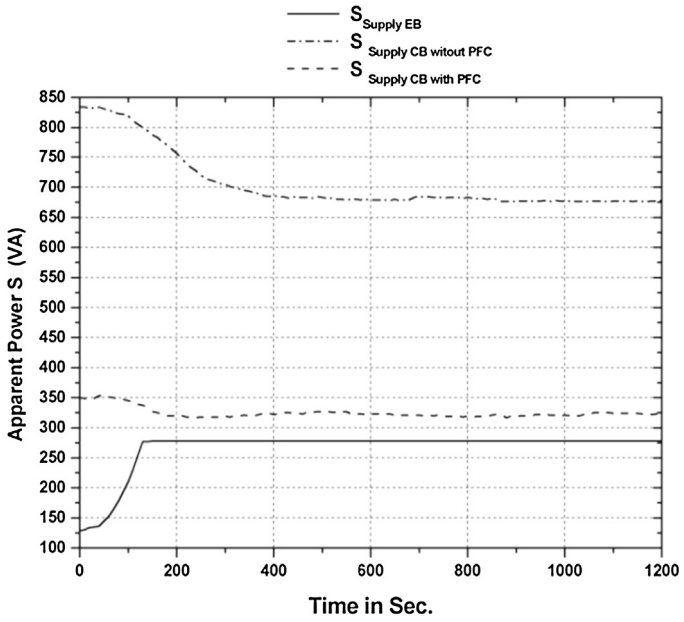

Fig. 29. Apparent power at the supply terminals.

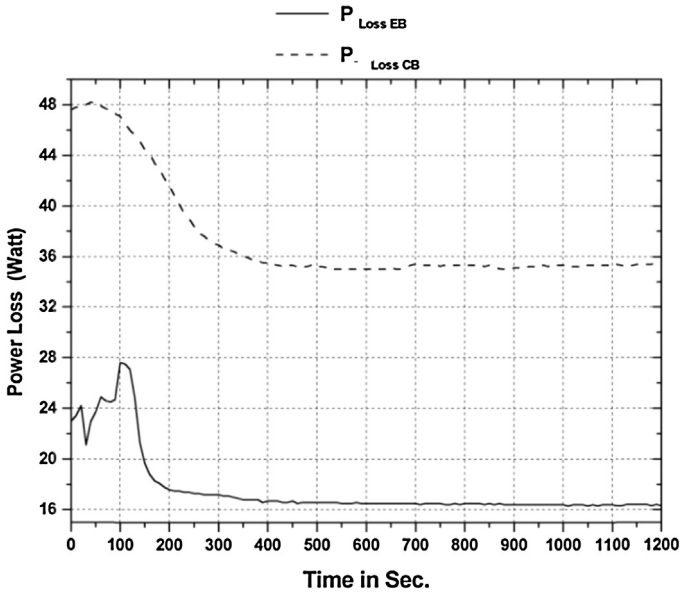

Fig. 30. Power losses comparison.

Fig. 29 shows that case 2 outperforms case 1 with respect to the total Volt Ampere required for feeding the assembly. The cost of keeping a defective capacitor in a CB assembly or running a CB without C_{PF} is seemingly prohibitive for utility grids in terms of unutilized installed Volt Amperes.

Fig. 30 shows that the power loss in case 2 is considerably less than that of case 1 (better than 50% loss reduction)

The PF at the lamp terminals for both cases is shown in Fig. 31. It is clear that case 2 offers superior performance where the lamp operates close to unity power factor due to the inherent purely resistive characteristics of the lamp and the good linearity of its resistance when it is fed by high frequency excitation.

In case 1, the lamp operates at 0.853 power factor, although it acts as a resistive load, its nonlinear characteristics results in harmonic voltages that adds harmonic reactive power and hence reducing the effective lamp power factor.

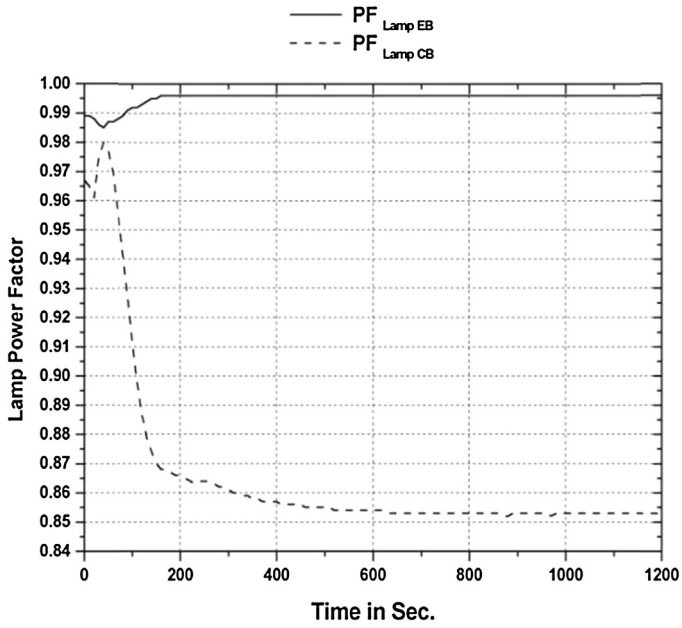

Fig. 31. PF at the lamp terminals.

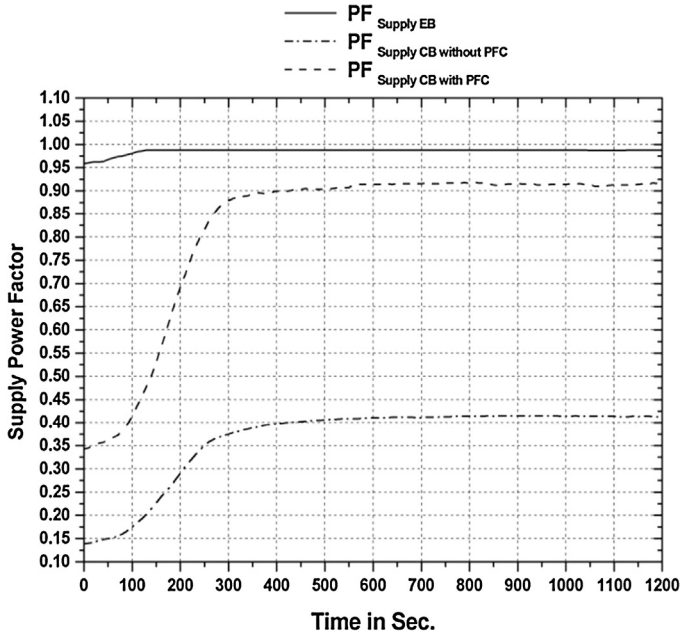

Fig. 32. PF at the supply terminals for EB and CB systems.

The power factor at the supply terminals for both ballast cases is shown in Fig. 32. It is clear that cases 1 without and with C_{PF} offer inferior performance to case 2. The CB without PFC has a starting power factor of 0.139 and improves to 0.413 at steady state. But with adding a PFC capacitor the power factor at starting is slightly improved to 0.343 and improves to 0.915 at steady state. EB is the best operating system for the HPS lamps since the power factor at the supply point is very high at starting which equal to 0.959 and rapidly improves to 0.988 as system approaches steady state.

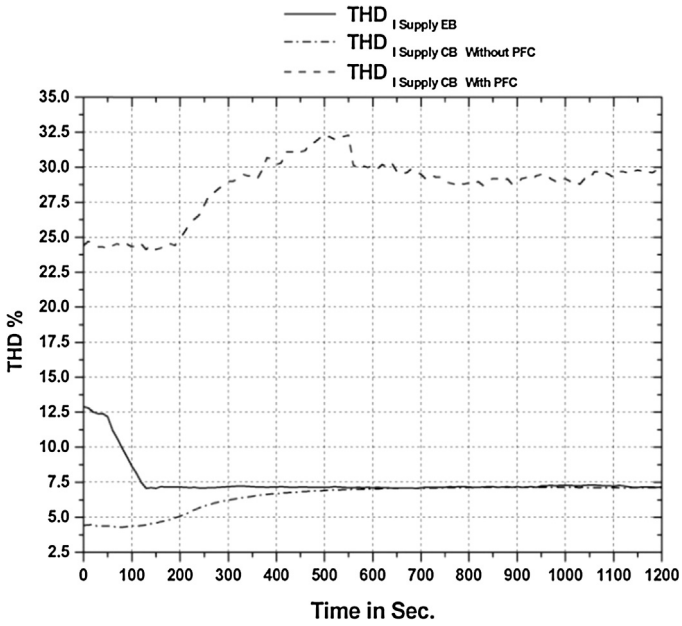

Fig. 33. Supply THD current for both EB and CB system.

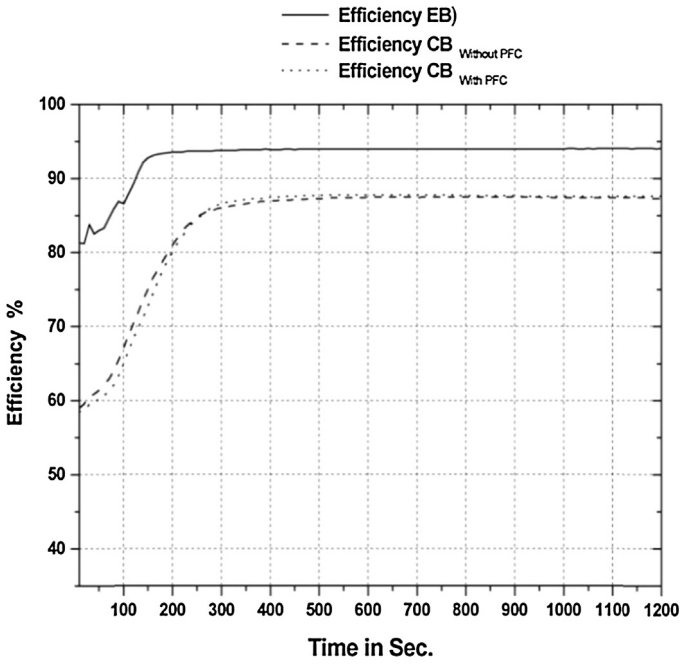

Fig. 34. Efficiency.

Fig. 33 shows the comparison between the THD of the current drawn by the assembly in the two cases. It is clear that case 2 has a THD of 7.16% in the steady state operation mode after a short transient interval (about 120 s) started by a THD of 12.5%, case 1 can give the same THD if the PFC capacitor is eliminated. This has been explained in Section 3. The cost of eliminating the PFC capacitor is prohibitive as inferred from Section 2 and 3.

Finally Fig. 34 shows that the efficiency in case 2 is far better than in case 1 (94.1% versus 87.3%). It is also shown that PFC capacitor may have very slight impact on overall efficiency of the lamp system itself; however, it improves the efficiency of the whole lighting network as it greatly reduces the transmission network losses.

Table 1
CB and EB operating conditions.

	CBWithout PFC	CBWith PFC	EB
V_{lamp} (V)	94.1	97.5	104.8
I_{lamp} (A)	3.1	3.1	2.5
I_{supply} (A)	3.1	1.4	1. 3
PF_{lamp}	0.853	0.851	0.996
PF_{supply}	0.413	0.915	0.988
P_{lamp} (W)	244.7	259.3	258.4
P_{supply} (W)	280.3	296.2	274.7
P_{loss} (W)	35.6	36.9	16.3
Q_{lamp} (VAR)	149.9	159.9	23.1
Q_{supply} (VAR)	617.7	130.7	43.8
S_{lamp} (VA)	286.98	304.64	259.47
S_{supply} (VA)	678.3	323.7	278.2
Efficiency (η %)	87.31	87.55	94.07

6. Conclusions

Table 1 summarizes the findings explored in the different sections of this study. It is concluded that the performance of a lighting system composed of a HPS lamp fed by electronic ballast is superior in almost all operational aspects to the system composed of the same lamp when fed through conventional electromagnetic ballast even if a power factor correction capacitor is provided. Superiority is attributed to substantial improvements in system power factor, efficiency, total harmonic distortion, and warming up period. Due to adaptive control of lamp power, the degraded performance associated with lamp aging that is observable when HPS lamps are fed by conventional ballast is entirely eliminated when electronic ballast is used. The degraded performance as reported in literature includes reduced lamp power due to increase in its operational resistance and possibility of ignition failure due to increase in breakdown voltage with aging. Another critical issue that has been tested and validated in this study is the ability of electronic ballast to maintain lamp power and to ensure ignition success across a wider regulation span of supply voltage, a feature that can be very decisive in ballast type selection for lighting networks suffering from wide voltage regulation band.

Finally the parameters of the conventional ballast assembly used are:

- Power factor correction capacitor $C_{PF} = 35\ \mu F$, 250 V
- CB parameters: ($L = 154$ mh, $R = 2.04\ \Omega$)

Acknowledgment

The authors are grateful to the Electronics Research Institute, Dokki, Cairo, Egypt for financing this research.

References

Ben-Yaakov, S., Gulko, M., 1997. Design and performance of an electronic ballast for high pressure sodium (HPS) lamp. IEEE Trans. Ind. Electron. 44 (August (4)), 486–491.

Branas, C., Azcondo, F.J., Bracho, S., 1998. Electronic ballast for HPS lamps with dimming control by variation of the switching frequency. Soft start-up method for HPS and fluorescent lamps. In: Proceedings of the 24th Annual Conference of the IEEE, Industrial Electronics Society, vol. 2, IECON '98, pp. 953–958.

Branas, C., Azcondo, F.J., Bracho, S., 2000. Contributions to the design and control of LC_sC_p resonant inverters to drive high-power HPS lamps. IEEE Trans. Ind. Electron. 47 (4), 796–808.

Cardesin, J., Calleja, A., Alonso, M., Corominas, E.L., Ribas, J., Rico-Secades, M., Garcia, J., 2003. Advanced design of a low-cost electronic ballast with PFC for HPS lamps. In: 38th IAS Annual Meeting Conference Record of the Industry Applications, vol. 1, 12–16 October, pp. 325–331.

Dorleijn, J.W.F., Vanderheijden, R.L.A., 1980. Properties of high-pressure sodium arcs at frequencies above 50 Hz. In: 33th Gaseous Electronics Conference, Oklahoma, paper LA-2.

Giezendanner, F., Biela, J., Kolar, J.W., 2014. Optimization and performance evaluation of an AC-chopper ballast for HPS lamps. IEEE Trans. Ind. Electron. 61 (5), 2236–2243.

Jeong, I.W., Rim, G.H., Lee, H.J., Ryoo, H.J., Kim, J.S., Lee, H.S., 2001. Development of an electronic ballast for 250 W HPS lamps. In: IEEE Proceedings of International Symposium on Industrial Electronics, ISIE, vol. 1, pp. 42–45.

Martin, F.J.F., Viejo, C.B., Anton, J.C.A., Garcia, M.A.P., Rico-Secades, M., Alonso, J.M., 2003. Analysis and design of a high power factor, single-stage electronic ballast for high-intensity discharge lamps. IEEE Trans. Power Electron. 18 (2), 558–569.

Martín, A., Bordel, N., Blanco, C., Alvarez Antón, J.C., Zissis, G., 2010. Comparison of the emission of a high-pressure sodium lamp working at 50 Hz and at high frequency. IEEE Trans. Ind. Appl. 46 (September/October (5)), 1740–1745.

Sincero, G., Franciosi, A.S., Perin, A.J., 2005. A 250 W high pressure sodium lamp high power factor electronic ballast using an AC chopper. In: 2005 European Conference on Power Electronics and Applications, pp. 1–10.